Transport and magnetic properties of $Ce_xLa_{1-x}Au_2$ ($0 \leq x \leq 0.7$) and $PrAu_2$

1989 J. Phys.: Condens. Matter 1 7913

(http://iopscience.iop.org/0953-8984/1/42/011)

J. Phys.: Condens. Matter 1 (1989) 7913–7920. Printed in the UK

Transport and magnetic properties of $Ce_xLa_{1-x}Au_2$ ($0 \leqslant x \leqslant 0.7$) and $PrAu_2$

Y Sugiyama
Department of Physics, Faculty of Science, Tokyo Metropolitan University, Fukazawa 2-1-1, Setagaya-ku, Tokyo, Japan

Received 6 December 1988, in final form 26 April 1989

Abstract. Transport and magnetic properties of $Ce_xLa_{1-x}Au_2$ ($0 \leqslant x \leqslant 0.7$) and $PrAu_2$ are measured between 1.6 K and 280 K. No Kondo-like behaviour is observed in the former. In both systems, the observed resistivity is understood by crystal-field-splitting scattering. The nature of the phase transitions at low temperature is discussed.

1. Introduction

Many interesting properties have been observed in the compounds of rare earths (RE) with other elements because of interaction of 4f electrons with conduction electrons. We report here new results on the transport and magnetic properties of $Ce_xLa_{1-x}Au_2$ and $PrAu_2$.

$RECu_2$ compounds have shown interesting behaviour, in particular heavy fermion character in $CeCu_2$ (Gratz *et al* 1985, Onuki *et al* 1985) and a Jahn–Teller transition in $PrCu_2$ (Ott *et al* 1977).

In $CeCu_2$, electrical resistivity and thermoelectric power (TEP) show the combined effect of Kondo scattering and crystal field (CF) effect. This compound also shows an anisotropic antiferromagnetic transition below 3.5 K.

In $PrCu_2$, the ground-state multiplet of Pr^{3+} splits into nine singlets in its crystal field. Below 7.3 K, the lowest two singlets increase their separation and the crystal undergoes a cooperative Jahn–Teller transition (Ott *et al* 1977). Nuclear antiferromagnetic transition of $PrCu_2$ takes place below 54 mK (Andres *et al* 1972, Kawarazaki and Arthur 1988).

Both $CeAu_2$ and $PrAu_2$ have the same crystal structure as $CeCu_2$ or $PrCu_2$ (orthorhombic: $CeCu_2$ type), and Cu and Au have the same valence. This makes it interesting to look at $CeAu_2$ and $PrAu_2$. A single-phase sample of $CeAu_2$, however, does not seem to form, but we can follow the same crystal structure as $CeCu_2$ up to $x = 0.7$ in $Ce_xLa_{1-x}Au_2$ system. $LaAu_2$ is selected as a reference compound since La has no 4f electron.

2. Experimental procedure

The polycrystalline samples of $Ce_xLa_{1-x}Au_2$ with $x = 0$, 0.1, 0.3, 0.5, 0.7 and $PrAu_2$ were prepared by arc-melting appropriate amounts of elements on a water-cooled

0953-8984/89/427913 + 08 $02.50

copper hearth in an argon atmosphere. The starting materials are 99.9% La, Ce, Pr and 99.99% Au. $Ce_xLa_{1-x}Au_2$ samples were annealed just below the melting temperature for two or three days. The $PrAu_2$ sample was annealed at 800 °C for a week. This annealing temperature for $PrAu_2$ was selected since the sample undergoes a structural phase transition just above this temperature (McMasters *et al* 1971). The lattice constants of $LaAu_2$ determined with x-ray powder method are $a = 4.811$ Å, $b = 7.218$ Å and $c = 8.324$ Å which agree with reported ones within 2% (Iandelli and Palenzona 1968) and those of $PrAu_2$ are $a = 4.687$ Å, $b = 7.257$ Å and $c = 8.081$ Å which agree with reported ones within 3% (McMasters *et al* 1971). Metallographic analysis using an optical microscope shows that the samples containing Ce have many microcracks. The typical sample size is about $10 \times 1.5 \times 0.4$ mm^3.

The electrical resistivity was measured by a conventional four-terminal DC method. The sample current is 100 mA.

TEP was measured by a conventional differential method with a thin copper wire as a reference. The absolute thermoelectric power of the reference copper wire was calibrated against pure Pb using the table of Roberts (1977). The temperautre difference, 0.5 K above 7 K and 7% of measuring temperature below 7 K, was measured with an Au + 0.07%Fe–chromel differential thermocouple. Thermoelectric voltages of sample and differential thermocouple were measured by two Keithley model 181 nanovoltmeters controlled by a microcomputer.

Magnetic susceptibility and magnetisation were measured by a low-frequency vibrating sample magnetometer in applied fields up to 11 kG.

3. Experimental results

Figure 1 shows the temperature dependence of resistivity $\rho(T)$ of $Ce_xLa_{1-x}Au_2$ and $PrAu_2$. The residual resistivity of $Ce_xLa_{1-x}Au_2$ increases with increasing Ce concentration. The residual resistivities ratio (RRR) of $LaAu_2$ and $PrAu_2$ are 36.6 and 10.0 respectively. Errors shown in the figure are mainly due to uncertainty in the sample size determination. From the temperature dependence of the resistivity we estimated the Debye temperature of $LaAu_2$ to be about 100 K, assuming a Bloch–Grüneisen term and an additional empirical term (Merlo and Canepa 1987). As clearly shown in figure 2, in the case of $Ce_xLa_{1-x}Au_2$ for $x = 0.3, 0.5, 0.7$ and $PrAu_2$, there is an additional reduction in the resistivity with decreasing temperature below 10 K, which suggests the presence of some phase transitions.

In order to see the magnetic part of resistivity, the resistivity of $LaAu_2$ was subtracted from those of $Ce_xLa_{1-x}Au_2$ and $PrAu_2$, and the results are shown in figure 3. The magnetic resistivity of $Ce_xLa_{1-x}Au_2$ decreases monotonically with decreasing temperature though the experimental errors are rather large. The curve of $PrAu_2$ increases up to 130 K with increasing temperature and above that temperature it is essentially constant within experimental error.

The temperature dependence of the TEP of $Ce_xLa_{1-x}Au_2$ is shown in figure 4. No drastic effect on TEP is produced by replacing La with Ce. Over the investigated temperature range, the TEP is relatively small and negative for all Ce concentrations. In $LaAu_2$, there is a hump near 25 K (indicated by an arrow) which might be due to the phonon drag effect.

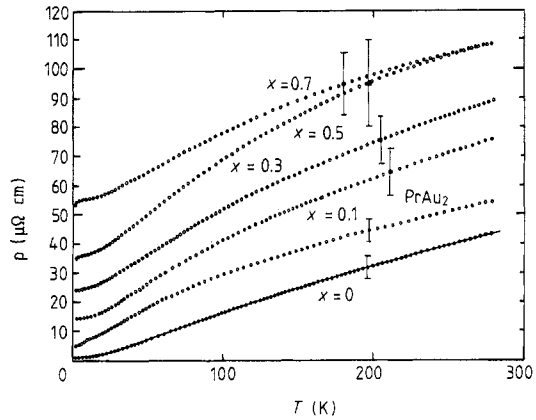

Figure 1. The electrical resistivity for $Ce_xLa_{1-x}Au_2$ ($x = 0, 0.1, 0.3, 0.5, 0.7$) and $PrAu_2$ as a function of temperature.

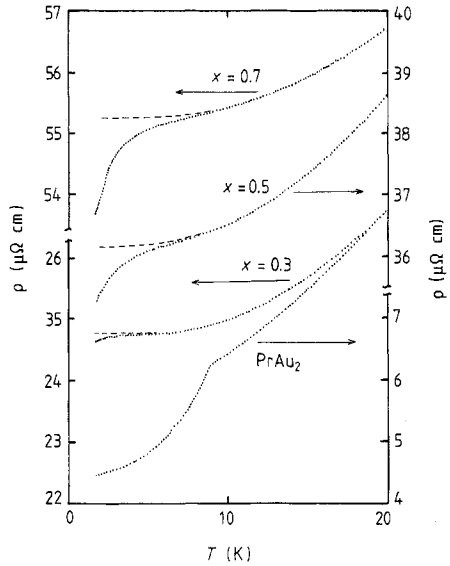

Figure 2. The temperature dependence of the electrical resistivity for $Ce_xLa_{1-x}Au_2$ ($x = 0.3, 0.5$ and 0.7) and $PrAu_2$ near the transition temperature. The broken curves show the phonon contribution extrapolated from the higher temperature region.

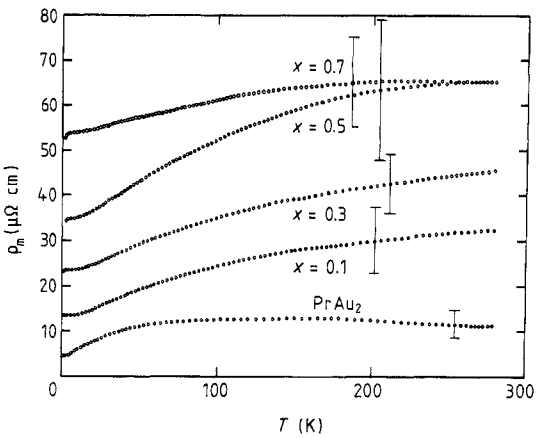

Figure 3. The magnetic part of the resistivity for $Ce_xLa_{1-x}Au_2$ ($x = 0.1, 0.3, 0.5, 0.7$) and $PrAu_2$ as a function of temperature.

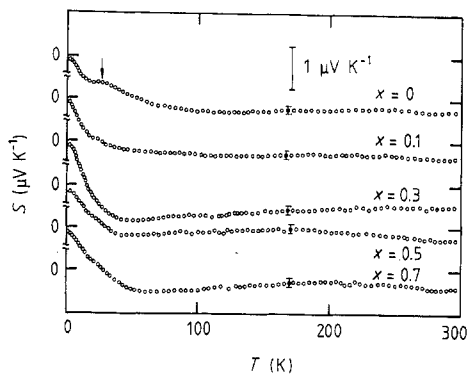

Figure 4. The thermoelectric power for $Ce_xLa_{1-x}Au_2$ ($x = 0, 0.1, 0.3, 0.5, 0.7$) as a function of temperature.

Figure 5 shows the TEP of $PrAu_2$ as a function of temperature. The TEP of this compound is also small and negative. There is a minimum near 17 K. We also find a kink near 8.5 K as clearly shown in the inset.

Figure 6 shows examples of the temperature dependence of the inverse magnetic susceptibility $\chi^{-1}(T)$ of $Ce_xLa_{1-x}Au_2$ and $PrAu_2$. $\chi(T)$ was measured at 8 kG in the high

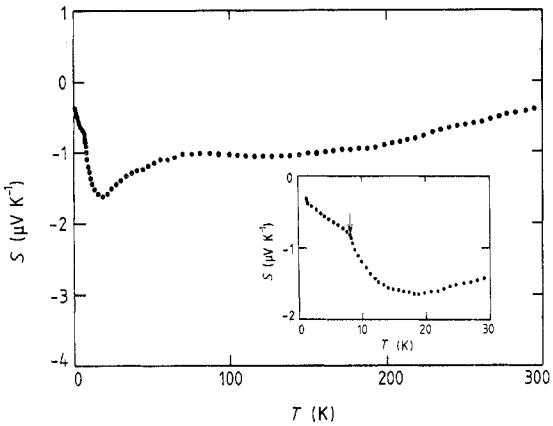

Figure 5. The thermoelectric power for $PrAu_2$ as a function of temperature. The inset shows an expanded view of the low temperature range.

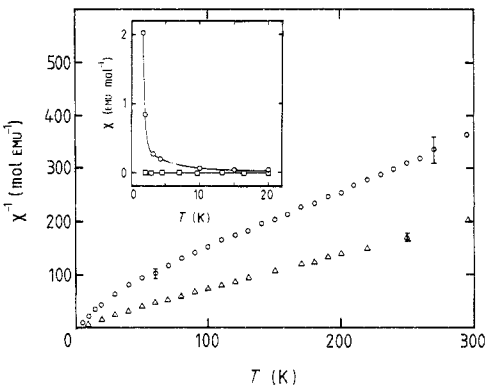

Figure 6. Reciprocal magnetic susceptibility for $Ce_{0.5}La_{0.5}Au_2$ (open circles) and $PrAu_2$ (triangles) as a function of temperature. The inset shows the magnetic susceptibility for $Ce_{0.5}La_{0.5}Au_2$ (circles) and $LaAu_2$ (squares) as a function of temperature for the lower temperature range.

temperature region, and in the low temperature region it was obtained from the slope of M at zero field. $\chi^{-1}(T)$ follows the Curie–Weiss law above approximately 100 K for $Ce_{0.5}La_{0.5}Au_2$ and $PrAu_2$. The effective Bohr magneton μ_{eff} and the paramagnetic Curie temperature θ_p of $Ce_{0.5}La_{0.5}Au_2$ are estimated to be $2.7 \pm 0.2\mu_B$ and -40 ± 10 K respectively. On other samples cut from the same ingot, we obtained a μ_B value in agreement with the above value within the experimental uncertainty; however, the estimated θ_p varies from -40 K to -90 K. One possible origin is the preferred grain orientation in the samples, since in $CeCu_2$ Onuki *et al* (1985) found large anisotropy in θ_p (+17 K, -25 K and -270 K for the a, b and c axes respectively).

The μ_{eff} and θ_p of $PrAu_2$ are estimated to be $3.5 \pm 0.1\mu_B$ and -10 ± 5 K respectively.

The inset of figure 6 shows the magnetic susceptibility $\chi(T)$ of $LaAu_2$ and $Ce_{0.5}La_{0.5}Au_2$ at low temperature. $\chi(T)$ of $LaAu_2$ is small and nearly temperature independent. $\chi(T)$ of $Ce_{0.5}La_{0.5}Au_2$ is still increasing steeply even at the lowest temperature.

Figure 7 shows the magnetisation M of $Ce_{0.5}La_{0.5}Au_2$ (a) and $PrAu_2$ (b). The lower the temperature, the more steeply the magnetisation of $Ce_{0.5}La_{0.5}Au_2$ increases with magnetic field at lower fields. Compared with the polycrystalline $CeCu_2$ (Gratz *et al* 1985), the magnetic moment per Ce atom of $Ce_{0.5}La_{0.5}Au_2$ at similar temperatures (1.5 K and 1.7 K) is about three times larger.

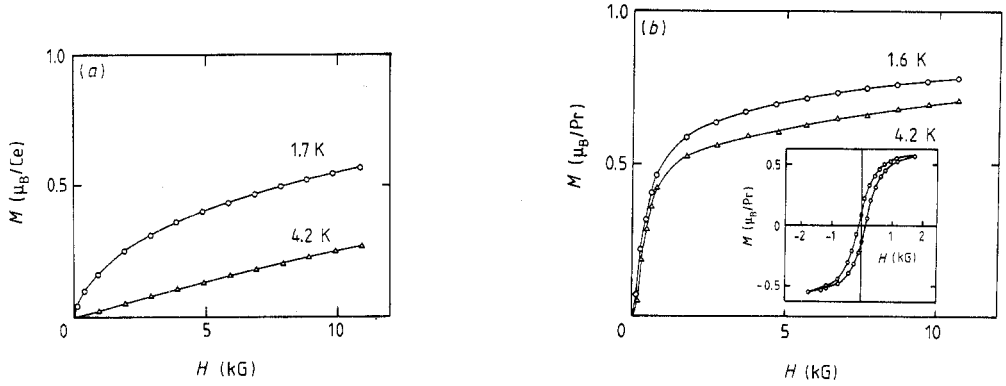

Figure 7. (*a*) The magnetisation for $Ce_{0.5}La_{0.5}Au_2$ as a function of magnetic field at 1.7 K and 4.2 K. (*b*) The magnetisation for $PrAu_2$ as a function of magnetic field at 1.6 K and 4.2 K. The inset shows an expanded view of the low temperature range.

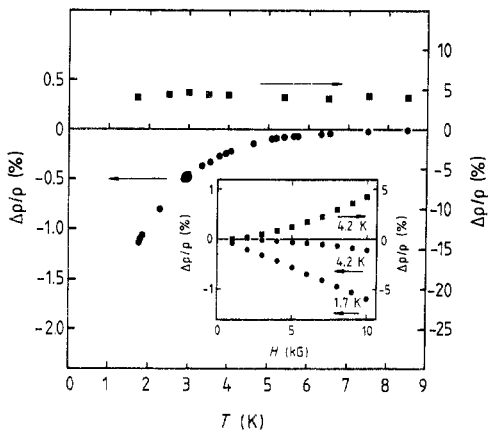

Figure 8. The magnetoresistance for $Ce_{0.5}La_{0.5}Au_2$ (circles) and $LaAu_2$ (squares) as a function of temperature at 10 kG. The inset shows the field dependence for $Ce_{0.5}La_{0.5}Au_2$ (circles) at 1.7 K and 4.2 K, and for $LaAu_2$ (squares) at 4.2 K.

The magnetisation of $PrAu_2$ increases steeply at lower fields and tends to saturate at higher fields. It shows hysteresis in the lower field region.

The temperature dependence of the magnetoresistance at 10 kG of $LaAu_2$ and $Ce_{0.5}La_{0.5}Au_2$ is shown in figure 8. The magnetoresistance of $LaAu_2$ is positive over the investigated temperature range. The magnetoresistance of $Ce_{0.5}La_{0.5}Au_2$ becomes negative below about 8 K and is still decreasing at 1.7 K with decreasing temperature.

4. Discussion

4.1. Absence of the Kondo effect in $Ce_xLa_{1-x}Au_2$

In figure 3 the magnetic part of resistivity of $Ce_xLa_{1-x}Au_2$ hardly shows any behaviour characteristic of the Kondo effect at any concentration. This is not only different from the case of $CeCu_2$ but a rather exceptional case among Ce compounds. The only other exception we know is Ce_2Zn_{17}, investigated by Sato *et al* (1988).

The Kondo effect is also not found in TEP (figure 4). Ce-based Kondo lattice materials have general characteristics in the temperature dependence of TEP (Jaccard and Sierro 1982, Gottwick *et al* 1987). A positive peak due to the competition between Kondo scattering and CF scattering has been found at relatively high temperatures (40–200 K). In many Kondo lattice substances, there is a negative peak near the Kondo temperature. The TEP of $CeCu_2$ also has this characteristic Kondo-like behaviour (Gratz *et al* 1985). On the other hand, the TEP of $Ce_xLa_{1-x}Au_2$ is always negative and does not show any such structure.

These results, together with the result of the susceptibility measurement, show that the Ce ion in these compounds is a stable trivalent state and the mixing of the 4f electron with the conduction electron is quite small.

4.2. The crystal field effect of $\rho(T)$ and TEP

In the absence of the Kondo effect, the CF inelastic scattering makes an important contribution to the magnetic resistivity of $Ce_xLa_{1-x}Au_2$. We fit the calculation to measured results. In the calculation, we approximate the CF Hamiltonian, taking the second-order terms (Hutchings 1964) into account, as follows

$$H_{CF} = B_2^0[3J_z^2 - J(J+1)] + B_2^2(J_+^2 + J_-^2) \tag{1}$$

where B_2^0 and B_2^2 are the CF parameters and J is the total angular momentum. For the interaction between a conduction electron and a 4f electron, we assume an exchange and a quadrupole Coulomb interaction (Fisk and Johnston 1977). The temperature dependence of the magnetic resistivity is expressed as

$$\rho_m(T) = \sum_i \left(x|\langle i'|\boldsymbol{s}\cdot\boldsymbol{J}|i\rangle|^2 + (1-x)\sum_m |\langle i'|y_2^m|i\rangle|^2 \right) p_i f_{ii'} \tag{2}$$

and

$$p_i = \exp(-E_i/k_B T) \Big/ \left(\sum_i \exp(-E_i/k_B T) \right)$$

$$f_{ii'} = 2/\{1 + \exp[-(E_i - E_{i'})]\}$$

where the $|i\rangle$ and E_i are the eigenstates and corresponding energy eigenvalues of (1) respectively, and the y_2^m are operator equivalents for $L = 2$. The first term in the bracket of (2) is the contribution from exchange scattering and the second is from quadrupole Coulomb scattering.

Figure 9 shows the temperature-dependent part of the magnetic resistivity normalised at 280 K and a calculated result of CF scattering. The fitting parameters and CF levels used in the calculation are given. We obtain an overall agreement between experiment and calculation.

The similar fitting for $PrAu_2$ also gives reasonable agreement as shown in figure 10.

The peak found in the TEP of $PrAu_2$ at about 17 K (figure 5) might be due to the CF effect, which was suggested by Takayama and Fulde (1975). According to them, a peak should appear at about $\Delta/3$–$\Delta/2$, where Δ is the CF splitting between the ground state and the first excited state. Δ, estimated to be 30–50 K from TEP, is consistent with the value obtained in figure 10.

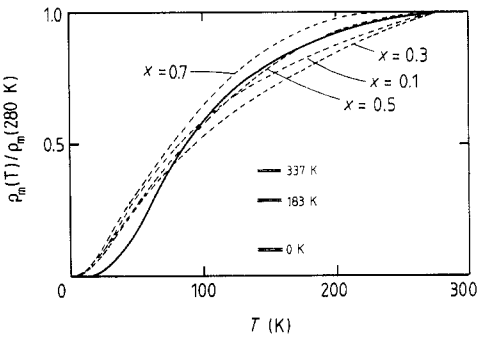

Figure 9. Calculated and measured temperature-dependent magnetic resistivities for $Ce_xLa_{1-x}Au_2$ ($x = 0.1, 0.3, 0.5, 0.7$) normalised at 280 K. The full curve is calculated for the indicated crystal field level scheme. The crystal field parameters are $B_2^0 = 25 \times 10^{-16}$ erg and $B_2^2 = 5 \times 10^{-16}$ erg, and the ratio of the aspherical Coulomb scattering to the exchange scattering at 280 K is 0.45.

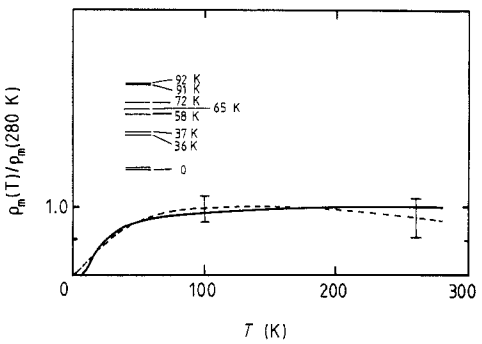

Figure 10. Calculated and measured temperature-dependent magnetic resistivities for $PrAu_2$ normalised at 280 K. The full curve is calculated for the indicated crystal field level scheme. The crystal field parameters are $B_2^0 = 1.9 \times 10^{-16}$ erg and $B_2^2 = 1.5 \times 10^{-16}$ erg, and the ratio of the aspherical Coulomb scattering to the exchange scattering at 280 K is 0.24.

4.3. Phase transitions at low temperature

Both systems $PrAu_2$ and $Ce_xLa_{1-x}Au_2$ ($x \geq 0.3$) show some phase transition at low temperature. In this subsection we discuss the magnetic state below the transition temperature.

In $PrAu_2$, the transition is ferromagnetic at 8.5 K approximately as clearly seen in the magnetisation (figure 7(*b*)) and transport properties (figures 2 and 5). It clearly means that exchange defeats the singlet ground state expected, an effect only found at much lower temperature and with the assistance of the hyperfine interaction in $PrCu_2$.

In the case of $Ce_xLa_{1-x}Au_2$, the features of transition near 5 K are not so simple.

(i) $\chi(T)$ at higher temperatures suggests antiferromagnetic character, but no cusp-like shape has been observed near T_c (figure 6).

(ii) At low temperatures, M at 10 kG is three times larger than that of antiferromagnetic $CeCu_2$.

(iii) In contrast to a typical ferromagnetic material, negative magnetoresistance does not show a minimum near T_c (figure 8).

This behaviour might be understood as an effect of magnetic clusters in a non-magnetic host due to short-range pair interaction between Ce moments. However, a definite explanation can not be given at the present time.

5. Conclusions

(i) Unlike many $Ce_xLa_{1-x}M_n$ systems, we find no Kondo effect in $Ce_xLa_{1-x}Au_2$ and conclude that the Ce^{3+} configuration is so stable that no negative exchange constant results from the mixing between the conduction electron and the 4f electron.

(ii) In both systems the magnetic part of resistivity was explained by CF scattering.

(iii) $PrAu_2$ shows the onset of ferromagnetism at 8.5 K approximately. $Ce_xLa_{1-x}Au_2$ ($x \geq 0.3$) also shows a magnetic phase transition where the transition temperature was

estimated to be 5 K approximately. The nature of the transition is not clear and more detailed investigations are required.

Acknowledgments

The author would like to thank Professor K Yonemitsu, Professor H Sato, Dr I Sakamoto and Dr I Shiozaki for stimulating discussions and a critical reading of this paper. He also thanks Professor Y Onuki and Professor N Sato for helpful suggestions. Moreover, he thanks Mr Takahara and Mr Huynh for their help in the measurements.

References

Andres K, Bucher E, Maita J P and Cooper A S 1972 *Phys. Rev. Lett.* **28** 1652
Fisk Z and Johnston D C 1977 *Solid State Commun.* **22** 359
Gottwick U, Held R, Sparn G, Steglich F, Vey K, Assmus W, Rietschel H, Stewart G R and Giorgi A L 1987 *J. Magn. Magn. Mater.* **63 & 64** 341
Gratz E, Bauer E, Barbara B, Zemirli S, Steglich F, Bredl C D and Lieke W 1985 *J. Phys. F: Met. Phys.* **15** 1975
Hutchings M T 1964 *Solid State Phys.* **16** 227 (New York: Academic)
Iandelli A and Palenzona A 1968 *J. Less-Common Met.* **15** 273
Jaccard D and Sierro J 1982 *Valence Instabilities* ed. P Wachter and H Boppart (Amsterdam: North-Holland) p 409
Kawarazaki S and Arthur J 1988 *J. Phys. Soc. Japan* **57** 1077
McMasters O D, Gschneidner K A, Bruzzone G and Palenzona A 1971 *J. Less-Common Met.* **25** 135
Merlo F and Canepa F 1987 *J. Phys. F: Met. Phys.* **17** 2373
Onuki Y, Machii Y, Shimizu Y, Komatsubara T and Fujita T 1985 *J. Phys. Soc. Japan* **54** 3562
Ott H R, Andres K, Wang P S, Wong Y H and Luthi B 1977 *Crystal Field Effects in Metals and Alloys* (New York: Plenum) p 84
Roberts R B 1977 *Phil. Mag.* **36** 91
Sato N, Kontani M, Hisashi A and Adachi K 1988 *J. Phys. Soc. Japan* **57** 1969
Takayama H and Fulde P 1975 *Z. Phys.* B **20** 81